

Improving Runoff Simulation in the Western United States with Noah-MP and VIC

Lu Su^{a,b}, Dennis P. Lettenmaier^b, Ming Pan^a, Benjamin Bass^c

^a Center for Western Weather and Water Extremes, Scripps Institution of Oceanography,
University of California, San Diego, United States

^b Department of Geography, University of California, Los Angeles, United States

^c Department of Atmospheric and Oceanic Sciences, University of California, Los Angeles,
United States

Correspondence: Dennis P. Lettenmaier (dlettenm@ucla.edu)

Abstract

Streamflow predictions are critical for managing water resources and for environmental conservation, especially in the water-short Western U.S. Land Surface Models (LSMs), such as the Variable Infiltration Capacity (VIC) model and the Noah-Multiparameterization (Noah-MP) play an essential role in providing comprehensive runoff predictions across the region. Virtually all LSMs require parameter estimation (calibration) to optimize their predictive capabilities. Here, we focus on the calibration of VIC and Noah-MP models at a 1/16° latitude-longitude resolution across the Western U.S. We first performed global optimal calibration of parameters for both models for 263 river basins in the region. We find that the calibration significantly improves the models' performance, with the median daily streamflow Kling-Gupta Efficiency (KGE) increasing from 0.37 to 0.70 for VIC, and from 0.22 to 0.54 for Noah-MP. In general, post-calibration model performance is higher for watersheds with relatively high precipitation and runoff ratios, and at lower elevations. At a second stage, we regionalize the river basin calibrations using the donor-basin method, which establishes transfer relationships for hydrologically similar basins, via

which we extend our calibration parameters to 4,816 HUC-10 basins across the region. Using the regionalized parameters, we show that the models' capabilities to simulate high and low flow conditions are substantially improved following calibration and regionalization. The refined parameter sets we developed are intended to support regional hydrological studies and hydrological assessments of climate change impacts.

1. Introduction

Streamflow predictions play a key role in water and environmental management, especially in the water-stressed Western U.S. (WUS). In the short term, these predictions provide early warnings for impending flood events, thereby enabling timely preparation and response to mitigate immediate flood risk and damages (Raff et al., 2013; Maidment, 2017). (In the longer term, streamflow predictions enable water utilities and agencies to plan water distribution within and across multiple uses—urban, agricultural, and industrial (Anghileri et al., 2016). Streamflow predictions also aid in understanding and foreseeing the impacts of climate change on water systems, thereby informing adaptive strategies for water resource management.

Streamflow predictions are derived via a synthesis of hydrometeorological data, statistical methodologies, and computational modeling. Direct measurement of runoff is an important element of this process, however it is only possible in river basins with well-developed observational infrastructure (Sharma and Machiwal, 2021). This limitation leaves vast areas, often critical to water resource management and climatology, without direct runoff observations on which to base streamflow predictions. As an alternative, Land Surface Models (LSMs) can be used to simulate streamflow. LSMs typically are forced with air temperature, precipitation and other surface meteorological variables. By integrating climatic, topographic, and land-use information, they can fill streamflow observation gaps and provide comprehensive,

spatially distributed runoff predictions (Fisher and Koven, 2020). The capabilities of LSMs equip us with the necessary tools to produce streamflow predictions that can be used to prepare for severe weather conditions, form the basis for water resource management, and inform water management associated with our evolving climate.

One of the key challenges in hydrological modeling is the reliable representation of the spatiotemporal variability of natural processes (Dembélé et al., 2020). Enhanced spatial resolution and improved estimates of surface meteorological variables have empowered LSMs to predict diverse processes with greater detail. However, a recurrent issue is that the parameters embedded in LSMs often inadequately capture fine-scale variations in land surface processes, as illustrated in Figures S7 and S8. Accurate prediction of land surface processes, particularly over large areas, requires accurate parameter estimation, which remains a significant bottleneck. Errors in parameter estimates affect LSMs' ability to forecast runoff at continental or subcontinental scales. Fisher and Koven (2020) identify LSM parameter estimation as one of three grand challenges in land surface modeling.

To deal with this challenge, we describe methods and resulting high-resolution parameter data sets for two widely used LSMs across the WUS. We base our estimates on a strategy of minimizing metrics of differences in observed and model-predicted streamflow, following many previous studies (Arsenault and Brissette, 2014; Poissant et al., 2017; Razavi and Coulibaly, 2017; Gochis et al., 2019; Qi et al., 2021 and Bass et al., 2023). We do so because streamflow observations are more readily available than other model prognostic variables like soil moisture or evapotranspiration (Demaria et al., 2007; Gao et al., 2018; Troy et al., 2008; Yadav et al., 2007), although the methods we use could be generalized to incorporate other observed and model-predicted fluxes and state variables. Although previous studies have mostly focused on a single hydrologic model (e.g., Mascaro et al. (2023),

Sofokleous et al. (2023), and Gou et al. (2020)), here we utilize two models to address structural model uncertainty and to ensure broader applicability of the calibration methods we employ.

The Variable Infiltration Capacity (VIC, Liang et al. (1994)) model and Noah-Multiparameterization (Noah-MP, Niu et al. (2011)), which we use here, are widely used hydrologic models both in the U.S. and globally, as highlighted by Mendoza et al. (2015) and Tangdamrongsub (2023). Many previous implementations of VIC for the Western United States (WUS) have been based on the Livneh et al. (2013) data set, and its predecessor, Maurer et al. (2002), which performed initial calibrations across the region. In the case of Noah-MP, Bass et al. (2023) performed manual calibration across the region. Neither of these implementations, however, employs globally optimized calibration, as we do here.

The process of calibration can be computationally demanding, and prior research typically has focused on obtaining parameters appropriate to facilitating model simulations that match observations as closely as possible at stream gauge locations (Duan et al,1992; Tolson and Shoemaker, 2007). Most previous studies have concentrated on a limited number of gauges/river basins (e.g. Mascaro et al. (2023); Sofokleous et al. (2023); and Gou et al. (2020)). Here, we aim to establish parameterizations for VIC and Noah-MP across the entire WUS. In doing so, we apply global optimization methods at 263 river basins, followed by a second stage regionalization to the whole of WUS.

Specifically, the work we report here aims to develop calibration parameters for the VIC and Noah-MP models that can be implemented at the catchment (Hydrologic Unit Code or HUC) 10 level across the region. We explore and elucidate (i) the choice of physical parameterizations and calibration of land surface parameters, (ii) extension of these calibrated parameters to areas without gauges, and (iii) factors that

influence calibration efficiency and LSM performance using regional parameter estimates. Following this introduction, Section 2 describes our calibration basins, the hydrologic models used, and the forcing dataset. The framework of our procedures is illustrated in Figure 1. Section 3 provides an in-depth exploration of the calibration process. In the case of Noah-MP, which offers multiple runoff generation (physics) options, our initial step involves choosing the most effective runoff parameterization option. Following this, we perform the calibration of land surface parameters. In the case of the VIC model, the runoff parameterization scheme is predetermined, so we commence immediately with calibration at 263 river basins across our region. Our second stage regionalization (section 4) extends the calibrated parameters to ungauged basins using the technique known as the donor basin method, as implemented by Bass et al. (2023). In Section 5, we evaluate both flood and low flow simulation skills both pre- and post-calibration, and following regionalization. Finally, following discussion and interpretation (section 6) section 7 presents conclusions, encapsulating the insights and implications of our study.

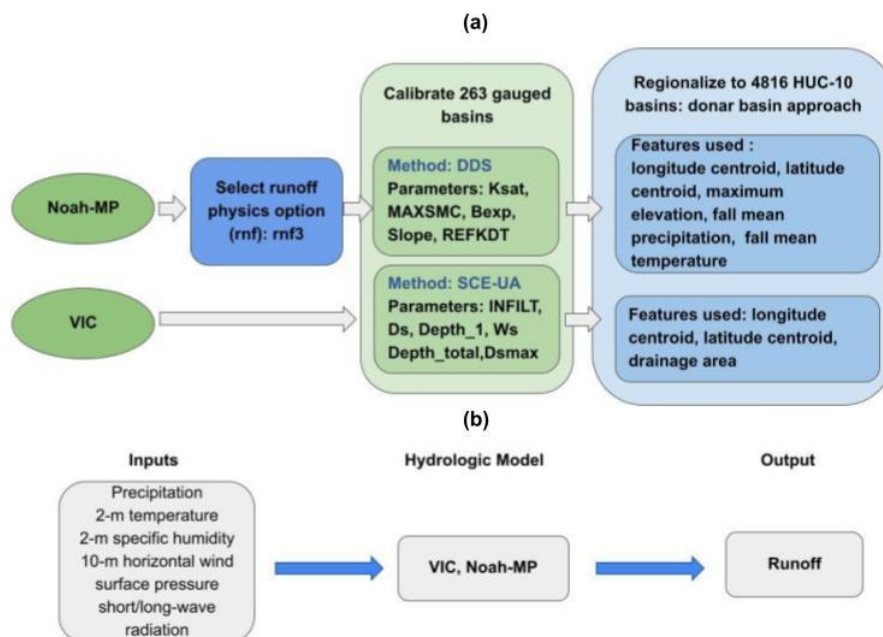


Figure 1 (a) framework of the calibration and regionalization processes adopted in this study. (b) model simulation inputs and output.

2. Study basins, land surface models and forcing dataset overview

2.1 Study Basins

We selected 263 river basins distributed across the WUS for calibration of the two models. Most of the basins were from USGS Gages II reference basins (Falcone 2011) which have minimum upstream anthropogenic effects such as dams and diversions. Among these basins, our selection criteria included having at least 20 years of record, and a minimum drainage area of 144 square kilometers, which is the size of four model grid cells. In addition to 250 Gages II reference stations, we included 13 basins located in California's Sierra Nevada for which naturalized flows (effects of upstream reservoir storage and/or diversions removed) are available from the California Department of Water Resources (2021). The locations of the 263 basins are shown in Figure 2. We used the most recent 20-year period of streamflow observations for calibration in each of the 263 basins.

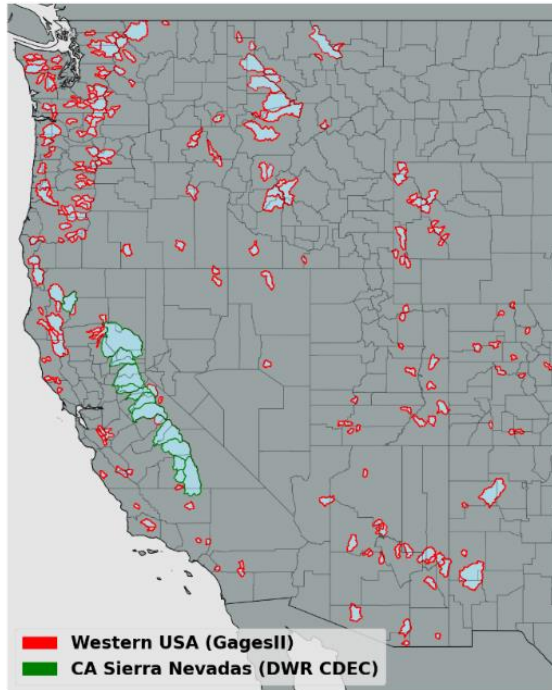


Figure. 2. 263 river basins for which calibration was performed. The Gages II reference basins are delineated with red boundaries and the CA Sierra Nevada basins with green boundaries.

2.2 Land Surface Models

The two models we used (VIC and Noah-MP) were chosen due to their broad application and proven effectiveness in hydrological simulations. The VIC model is renowned globally for its success in runoff simulation, as evidenced by studies such as Adam et al. (2003 & 2006), Livneh et al. (2013), and Schaperow et al. (2021). Conversely, Noah-MP, though relatively newer, forms the hydrologic core of the U.S. National Water Model (NWM) and is increasingly used both within the U.S. and abroad.

Our selection is further reinforced by a study conducted by Cai et al. (2014), which assessed the hydrologic performance of four LSMs in the United States using the North American Land Data Assimilation System (NLDAS) test bed. This study

highlighted Noah-MP's proficiency in soil moisture simulation and its strong performance in Total Water Storage (TWS) simulations, while recognizing VIC's capabilities in streamflow simulations.

Our choice of models also was informed by the varying levels of complexity these two models offer in conceptualizing the effects of vegetation, soil, and seasonal snowpack on the land surface energy and water balances (refer to Table 1 for more details). VIC and Noah-MP employ different parameterizations for various hydrological processes, such as canopy water storage, base flow, and runoff. Noah-MP features four runoff physics options (see Table 1). It utilizes four soil layers, each with a fixed depth. In contrast, the VIC model, with its variable infiltration capacity approach (Liang et al., 1994), uses up to three soil layers per grid cell with variable depths, providing flexibility in modeling soil moisture dynamics. The unique runoff generation methodologies of each model are particularly pertinent for capturing the diverse hydrological characteristics of the WUS.

The calibrated parameters we develop here for both models will provide future researchers with essential tools for comprehensive hydrological analysis across the WUS. Utilizing these two distinct models, each with unique strengths and methods, will facilitate thorough exploration of the WUS's varied hydrological characteristics, and response of the watersheds in the region to climate change, as well as implementation of improved streamflow forecast methods. Our results will help to facilitate a deeper understanding of hydrological processes and spatial variability across the entire WUS region.

In our implementation of both models, we accumulated runoff over each of the calibration watersheds. We chose not to implement the channel routing schemes of either model since their impact on daily streamflow simulations is small given the relatively small size of most of the basins. This aligns with earlier research (e.g., Li et

al. 2019). However, in both the case of VIC and Noah-MP, the output of our simulations (runoff) could be used as input to routing models, such as those that are options in the implementation of both models. We describe below the particulars of the two models.

2.2.1 VIC

VIC is a macroscale, semi-distributed hydrologic model (described in detail by Liang et al 1994) that determines land surface moisture and energy states and fluxes by solving the surface water and energy balances. VIC is a research model and in its various forms it has been employed to study many major river basins worldwide (e.g. Adam et al 2003 & 2006; Livneh et al 2013; Schaperow et al 2021). This model enjoys a broad user community — as per the citation index Web of Science, the initial VIC paper has been referenced more than 2600 times, with contributing authors spanning at least 56 different countries (Schaperow et al 2021). We obtained initial VIC model parameters from Livneh et al 2013, who validated model discharges over major CONUS river basins. The origins of the soil and land cover data are outlined in Table 1. The version of the VIC model implemented here is 4.1.2, and it operates in energy balance mode. We selected VIC 4.1.2 for two key reasons: First, our initial parameters were based on Livneh et al. (2013), who validated model discharges over major CONUS river basins using this model version. Second, in a preliminary assessment of snow water equivalent (SWE) simulation skills at select SNOTEL sites across the WUS, we found that VIC 4.1.2 demonstrated superior performance compared to VIC 5 (see Figure S1). This finding, coupled with our research group's extensive experience and proven results with VIC 4.1.2, informed our decision to use this version.

2.2.2 Noah-MP

Noah-MP was originally designed as the land surface scheme for numerical weather prediction (NWP) models like the Weather Research and Forecasting (WRF) regional atmospheric model. Currently, it's being utilized for physically based, spatially-distributed hydrological simulations as a component of the National Water Model (NWM) (NOAA, 2016). It enhances the functionalities of the Noah LSM (as per Chen et al., 1996 and Chen and Dudhia, 2001) previously used in NOAA's suite of numerical weather prediction models by offering multiple options for key processes that control land-atmosphere transfers of moisture and energy. These include surface water infiltration, runoff, evapotranspiration, groundwater movement, and channel routing (see Niu et al., 2007; 2011). The model has been widely used for forecasting seasonal climate, weather, droughts, and floods not only across the continental United States (CONUS) but also globally (Zheng et al., 2019). We utilized the most current version (WRF-HYDRO 5.2.0)

2.3 Forcing Dataset

We ran both models at a 3-hour time step and at $1/16^\circ$ latitude-longitude spatial resolution. The forcings were the gridded observation dataset developed by Livneh et al (2013) and extended to 2018 by Su et al (2021) (hereafter referred to as L13). This data set spans the period from 1915 to 2018. For the VIC model, the L13 dataset provided daily values of precipitation, maximum and minimum temperatures, and wind speed (additional variables used by VIC including downward solar and longwave radiation, and specific humidity, are computed internally using MTCLIM algorithms as described by Bohn et al. (2013)). The Noah-MP model, on the other hand, necessitated additional meteorological data such as specific humidity, surface

pressure, and downward solar and longwave radiation, in addition to precipitation, wind speed, and air temperature. We used the MTCLIM algorithms, as detailed by Bohn et al. (2013), to calculate specific humidity and downward solar radiation. We employed the Prata (1996) algorithm to compute the downward longwave radiation. Additionally, we deduced surface air pressure by considering the grid cell elevation in conjunction with standard global pressure lapse rates. Following this, we transitioned the daily data to hourly metrics using a cubic spline to interpolate between Tmax and Tmin, and derived other variables using the methods explained by Bohn et al. (2013). Lastly, we distributed the daily precipitation evenly across three hourly intervals.

We used a 3-hour simulation timestep given numerical considerations with Noah-MP (which don't affect VIC, however for consistency we used a 3-hour timestep for VIC as well. Despite the fact that precipitation in particular was available daily (and hence apportioned equally to 3-hour timesteps) resolving the diurnal cycle is sometimes important in the case of snow (accumulation and ablation) processes which vary diurnally.

Table 1. Overview of hydrologic model components and parameter data sources.

MODEL	SNOW ACCUMU LATION AND MELT	MOISTURE IN THE SOIL AND COLUMN/SURFACE RUNOFF	BASE FLOW	CANOPY STORAGE	VEGETAT ION DATA	SOIL DATA
VIC (V4.1.2)	Two-layer energy–mass balance model	Infiltration capacity function. Vertical movement of moisture through soil follows 1D Richards equation.	A function of the soil moisture in the third layer. Linear below a soil moisture threshold and becomes nonlinear above that threshold. [Liang et al., 1994]	Mosaic representation of different vegetation coverages at each cell.	University of Maryland 1-km Global Land Cover Classification (Hansen et al. 2000)	1-km STAT SGO database (Miller and White 1998).
NOAH-MP (WRF-HYDRO 5.2.0)	Three-layer energy–mass balance model that represents percolation	(1) TOPMODEL-based runoff scheme (2) Simple TOPMODEL-based runoff scheme with an equilibrium	Simple groundwater (hereafter SIMGM) [Niu et al., 2007]. Similar to SIMGM, but with a sealed bottom of the soil column [Niu et al.,	Semi-tile approach for computing longwave, latent heat, sensible heat and ground heat	MODIS 30-second Modified IGBP 20-category land cover product	1-km STAT SGO database (Miller and White

	, retention, and refreezing of meltwater within the snowpack.	water table (hereafter SIMTOP)	2005]	fluxes	1998).
		(3) Infiltration-excess-based surface runoff scheme	Gravitational free-drainage subsurface runoff scheme [Schaake et al., 1996]		
		(4) BATS runoff scheme, which parameterized surface runoff as a 4th power function of the top 2 m soil wetness (degree of saturation)	Gravitational free drainage [Dickinson et al., 1993]		

3. Model calibration

3.1 Calibration methods

The initial step in our calibration effort was to optimize the land surface parameters of the two models for the 263 WUS basins. These parameters, primarily soil properties which can exhibit a substantial degree of uncertainty, were iteratively updated via hundreds of simulations to accurately reflect streamflow conditions in each basin.

Our focus on calibrating soil-related parameters was based on their critical role in runoff generation. In this respect, we focused on key processes including infiltration, soil moisture storage, and groundwater recharge. The calibration of parameters that control these processes was prioritized to improve the representation of soil-water interactions, a major driver of runoff variability in the region. Given the importance of snow processes across much of the region, we conducted snow simulation verification at 20 Snow Telemetry (SNOTEL) (Natural Resources Conservation Service, 2023) sites across WUS. Our assessment (see Figure S1) indicated that the existing parameterizations for snow processes in both models reproduced observed SWE well across our study region.

Prior to calibration, we conducted a sensitivity analysis to identify the most

influential parameters for streamflow simulation in both models. We also drew on insights from previous research in this respect (Mendoza et al. 2015; Hussein 2020; Shi et al. 2008; Holtzman et al., 2020; Bass et al., 2023; Schaperow et al., 2023). We then performed a sensitivity analysis, focusing on how variations in the most sensitive parameters impacted Kling-Gupta Efficiency (KGE; Gupta et al., 2009). Based on these analyses, we chose to calibrate six parameters for the VIC model and five for the Noah-MP model (Table 2). For each parameter, we defined a physically viable range (refer to Table 2), drawing from values utilized in prior studies (Cai et al. 2014; Mendoza et al. 2015; Hussein 2020; Shi et al. 2008; Gochis et al., 2019; Holtzman et al., 2020; Lahmers et al. 2021; Bass et al., 2023; Schaperow et al., 2023).

In recent years, the development of hydrologic model calibration has evolved from manual, trial-and-error approaches to advanced automated techniques. This has included a shift towards global optimization methods, notably the Shuffled Complex Evolution algorithm (SCE-UA; Duan et al., 1992). Typically, SCE-UA has been applied to computationally efficient models (simulation time often on the order of a few minutes or less; see e.g., Franchini et al. (1998)). However, its application becomes less practical with more recent distributed hydrologic models such as the Noah-MP which require longer simulation times. To address these computational challenges, Tolson and Shoemaker (2007) introduced the Dynamically Dimensioned Search (DDS) algorithm, tailored for complex, high-dimensional problems. DDS is more computationally efficient than SCE-UA, and we therefore used it for our Noah-MP calibrations.

To assure that the parameter sets we estimated weren't dependent on the optimization method, we conducted a comparison between SCE-UA and DDS for calibrating VIC across 20 randomly chosen basins. We found that the DDS algorithm achieved optimal calibration with fewer iterations (typically around 3000 iterations vs

only about 250 for DDS). The parameter sets identified were nearly identical, affirming our decision to use distinct algorithms tailored to the computational demands of each model.

For both models, our objective function was the KGE metric for daily streamflow. KGE is a widely used performance measure because of its advantages in orthogonally considering bias, correlation and variability (Knoben et al., 2019). KGE = 1 indicates perfect agreement between simulations and observations; KGE values greater than -0.41 indicate that a model improves upon the mean flow benchmark (Konben et al., 2019).

TABLE 2. Calibration methods, parameters and modifications to their initial default values evaluated in the calibration.

Model	VIC		Noah-MP	
Calibration Method	SCE-UA		DDS	
Iterations	3000		250	
Calibrated Parameter	Variable Infiltration Curve Parameter (INFILT)	0.001 – 0.4 (Shi et al.,2008)	Saturated Hydraulic Conductivity (Ksat)	2×10^{-9} to 0.07 (Cai et al.,2014)
	Baseflow parameter (Ds)	0.001 – 1.0 (Shi et al.,2008)	Saturation soil moisture content (MAXSMC)	0.1 to 0.71 (Cai et al.,2014)
	Thickness of Soil in Layer 1 (Depth_1)	0.01 – 0.2 (Shi et al.,2008)	Pore size distribution index (Bexp)	1.12 to 22 (Cai et al.,2014; Gochis et al.,2019)
	Total thickness of soil column (Depth_total)	0.6 – 3.5 (Shi et al.,2008)	Linear scaling of “openness” of bottom drainage boundary (Slope)	0.1-1 (Lahmers et al 2021)
	Max velocity parameter of baseflow (Dsmax)	0.001 – 30 (Schaperow et al.,2023)	Parameter in surface runoff (REFKDT)	0.1-10 (Lahmers et al 2021)
	Fraction of max	0.001 – 1		

soil moisture where nonlinear baseflow occurs (Ws)	(Shi et al.,2008)
---	----------------------

3.2 Noah-MP parameterization

As specified in Table 1, Noah-MP has four runoff and groundwater physics options (rnf). Initially, we adopted the options that are incorporated in the NWM, as elaborated in Gochis et al. (2020). Before we could proceed with calibrating Noah-MP for all the WUS basins, it was necessary to determine suitable rnfs. To streamline computational time, we initially selected 50 basins randomly from the total of 263 from which we created four experimental groups. Each group employed a different rnf option. We applied the DDS method to these groups and compared the cumulative distribution functions (CDF) of their baseline and calibrated KGEs (Figure 3). From this figure, it's apparent that the KGE improved post-calibration for all four rnfs. Notably, rnf3, also known as free drainage, exhibited the most substantial performance enhancement after calibration. As a result, we chose to continue using this option which is incorporated in the NWM. Nonetheless, it's worth noting that the use of different options for different basins—a feature currently not utilized in Noah-MP or WRF-Hydro—could potentially result in improved overall model performance.

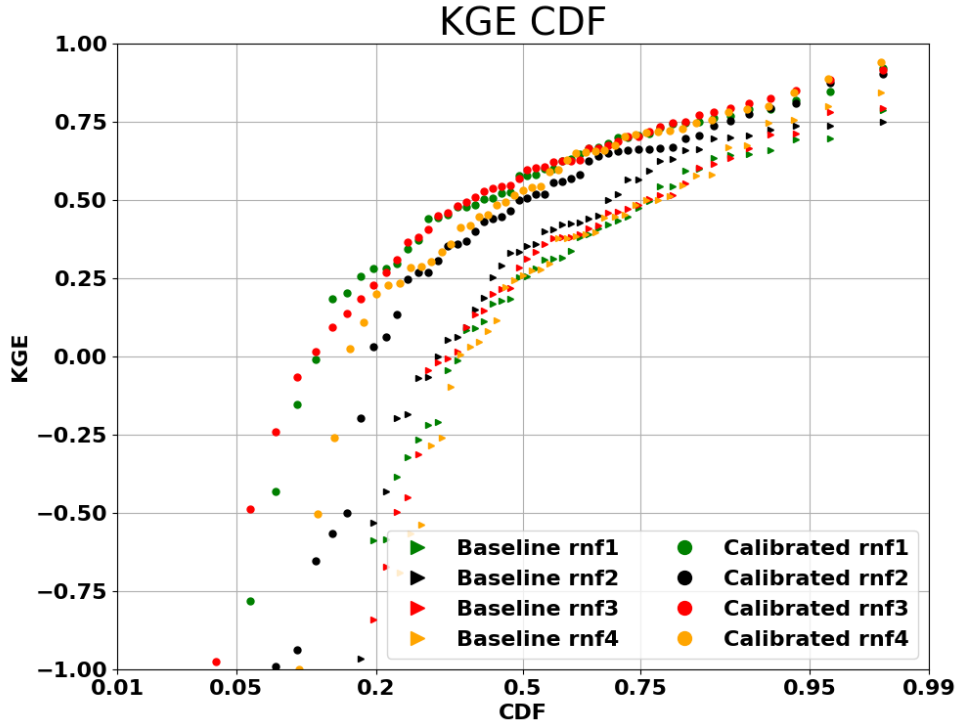


Figure 3. Streamflow performance (KGE of daily streamflow simulations) of different Noah-MP runoff generation options across 50 (of 263) randomly selected basins. The performances are shown for both baseline and calibrated simulations.

3.3 Calibration of gauged basins

Following the selection of the most effective set of runoff generation options across the domain, we estimated model parameters for all 263 basins. The comparative performance of the models, before and after calibration, is shown in Figure 4. It's apparent from the figure that both Noah-MP and VIC have significantly enhanced their daily streamflow simulation skills post-calibration. After calibration, the median KGE of Noah-MP improved from 0.22 to 0.54, and the VIC's median KGE increased from 0.37 to 0.70. When contrasting the two models, we observed that VIC outperformed Noah-MP both pre- and post-calibration. One possible explanation could be that the baseline VIC parameters were taken from Livneh et al. (2013), and these parameters had already been validated and adjusted for major U.S. basins

(although not for our 263 basins specifically), while the Noah-MP parameters are default values from NWM. Another possibility is inherent differences in the physics of streamflow simulation between the two models (VIC primarily generates runoff via the saturation excess mechanism), although that isn't the main focus of our research.

Following the calibration with data from the past 20 years, we performed a test where we calibrated the streamflow using the first 10 years of data and validated with the subsequent 10 years of data. This test revealed that the KGE distribution from the 10-year calibration is similar to that from the 20-year data. The median KGE values for VIC and Noah-MP after calibration with 10 years of observations were 0.52 and 0.69, respectively. Correspondingly, the median KGEs during the validation period were 0.50 and 0.68, respectively, which are only slightly lower. These comparisons demonstrate general consistency over time in the performance of the calibrated parameters.

To validate the robustness of our calibration methodology, we calculated alternative (to KGE) performance metrics, specifically Nash-Sutcliffe Efficiency (NSE) and bias. Our analyses, detailed in Figures S2&3, revealed significant enhancements in model performance as measured by these metrics. The observed improvements across multiple evaluation criteria affirm the efficacy of our calibration process, and in particular that the performance of our procedures is not contingent upon the choice of evaluation metrics.

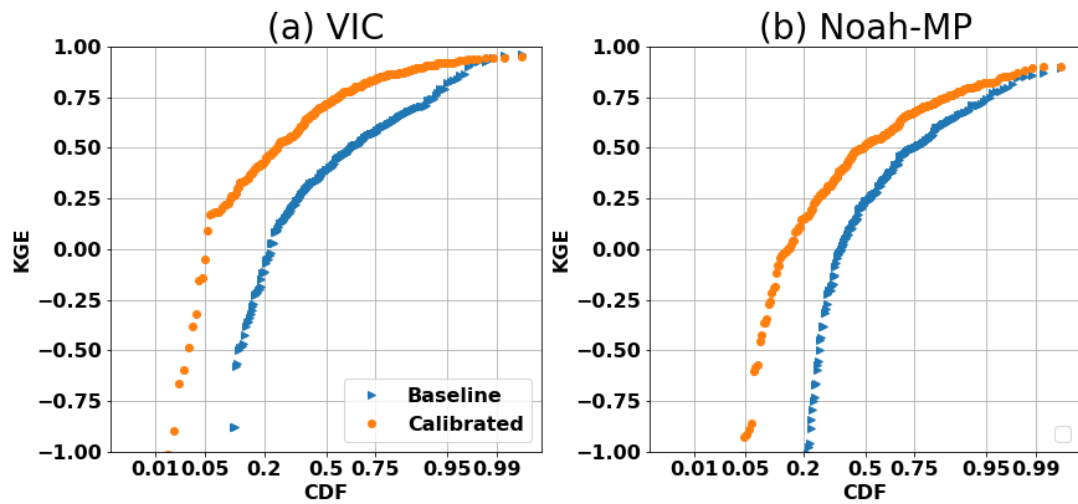


Figure 4. Cumulative Distribution Function (CDF) plot of the daily streamflow KGE for (a) VIC and (b) Noah-MP, comparing baseline and calibrated runs across all 263 basins.

We examined the spatial variability of daily streamflow KGE for Noah-MP and VIC, both before and after the calibration (see Figure 5). The highest baseline KGEs are along the Pacific Coast, in central to northern CA for both models. VIC's baseline KGE generally is high in the Pacific Northwest. Post-calibration improvements occurred for both models in most areas, especially in regions where the baseline KGE was low, such as southern CA and the southeastern part of the study region. Median improvements after calibration were 0.27 for Noah-MP and 0.30 for VIC.

We observed that basins displaying higher KGE values typically were more humid than those with lower KGE. To further delve into the relationship between KGE and basin characteristics, we explored correlations between KGE and 21 different characteristics, including drainage area, elevation, seasonal/annual average temperature and precipitation, annual maximum precipitation, and seasonal/annual runoff ratio. Of these, 12 characteristics were statistically significantly correlated with the VIC KGE, including four seasonal and annual runoff ratios; mean precipitation in winter, spring, and fall; annual maximum precipitation; and minimum elevation.

Figure 6 shows scatterplots of eight representative characteristics. Apart from minimum elevation and mean summer temperature, all other characteristics were positively correlated with KGE. Typically, spring runoff ratio, annual runoff ratio, mean annual max precipitation, and mean winter precipitation exhibited the highest correlations with KGE. This implies that basins with higher runoff ratios (particularly in spring), higher precipitation (especially maximum precipitation), lower summer temperature, and lower elevation are more likely to exhibit strong VIC performance. The same applies to Noah-MP, as indicated in Figure 7, although Noah-MP showed relatively weaker correlations. Correlations between mean summer temperature and mean fall precipitation and Noah-MP KGE weren't statistically significant.

The spatial distribution of the eight characteristics is qualitatively similar with the KGE spatial distribution, as shown in Figure 8. Generally, basins with higher KGE have higher characteristic values when the correlation is positive, and lower characteristic values when the correlation is negative. As noted above, both models show good baseline performance along the Pacific Coast, and in central to northern CA (Figure 5). Those areas have high runoff ratios (specifically spring and annual) and high mean winter precipitation. These features generally lead to runoff physics that are dominated by the saturation-excess mechanism, which is well represented by both VIC and Noah-MP. VIC's baseline KGE generally is high in the inland Northwest which has somewhat lower runoff ratios and (relatively) deeper groundwater tables. VIC's superior performance relative to Noah-MP may also be because of its variable rather than fixed soil moisture depths (as is the case for Noah-MP).

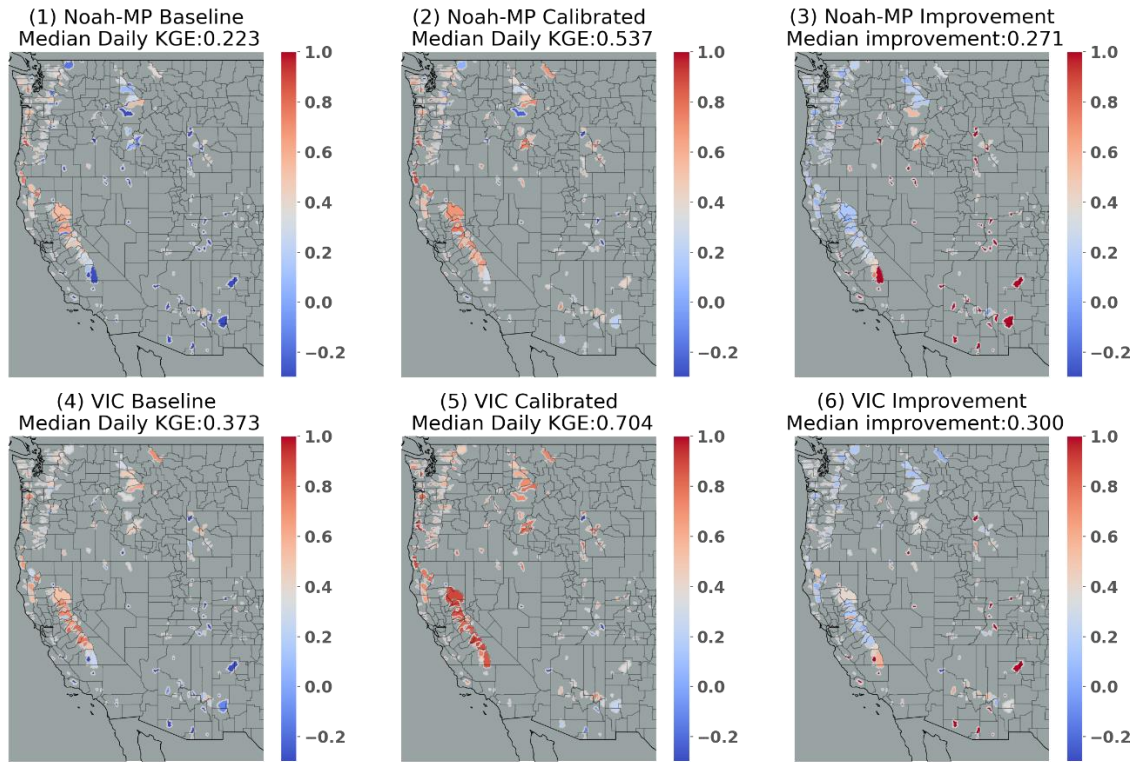


Figure 5. Spatial distribution of daily streamflow KGE for Noah-MP baseline (1); calibrated Noah-MP (2); difference between calibrated and baseline Noah-MP (3); VIC baseline (4); calibrated VIC (5); difference between calibrated and baseline VIC (6).

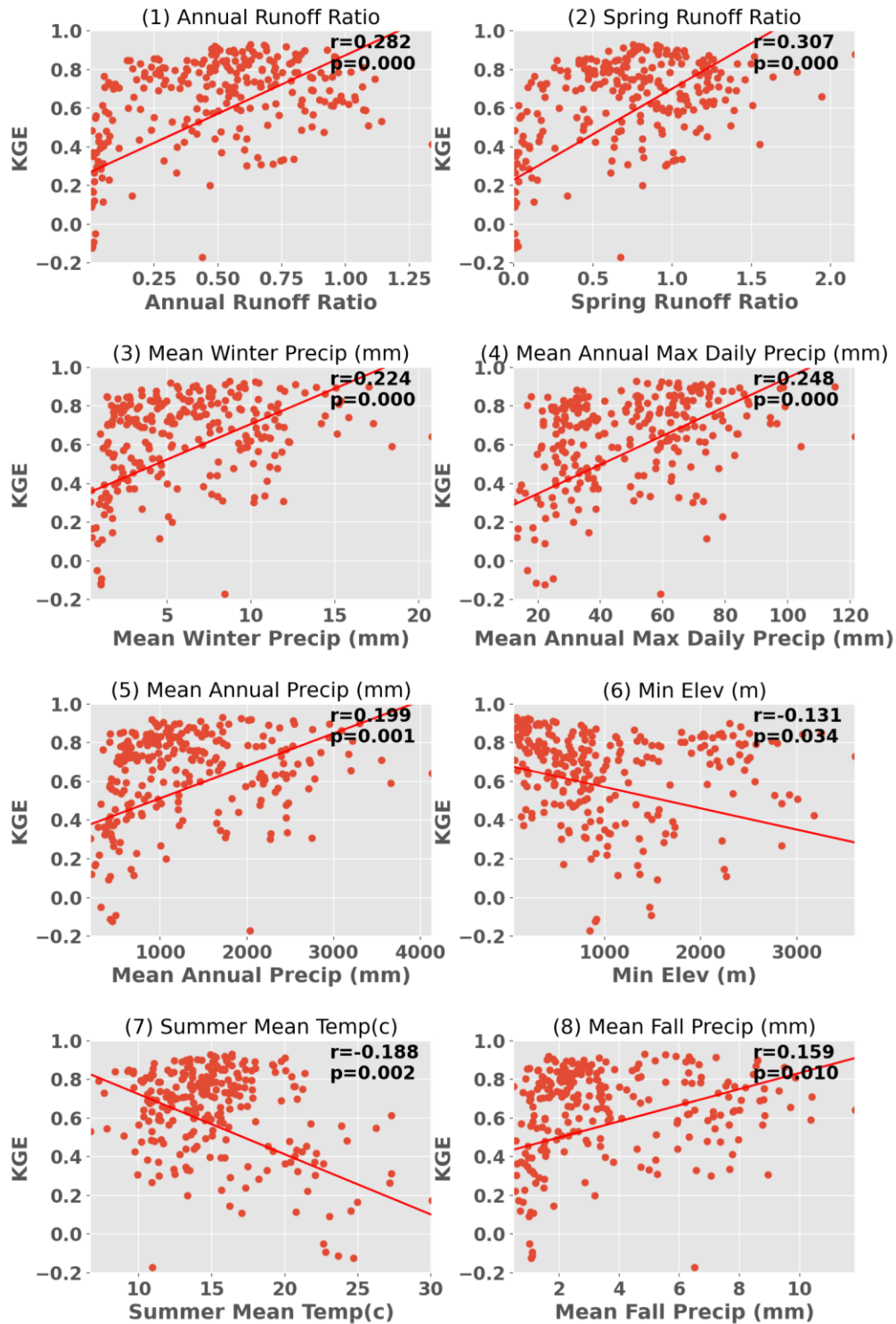


Figure 6. Scatterplots of VIC KGE in relation to significantly correlated characteristics. Each subplot indicates the corresponding Pearson correlation coefficients and the P-value.

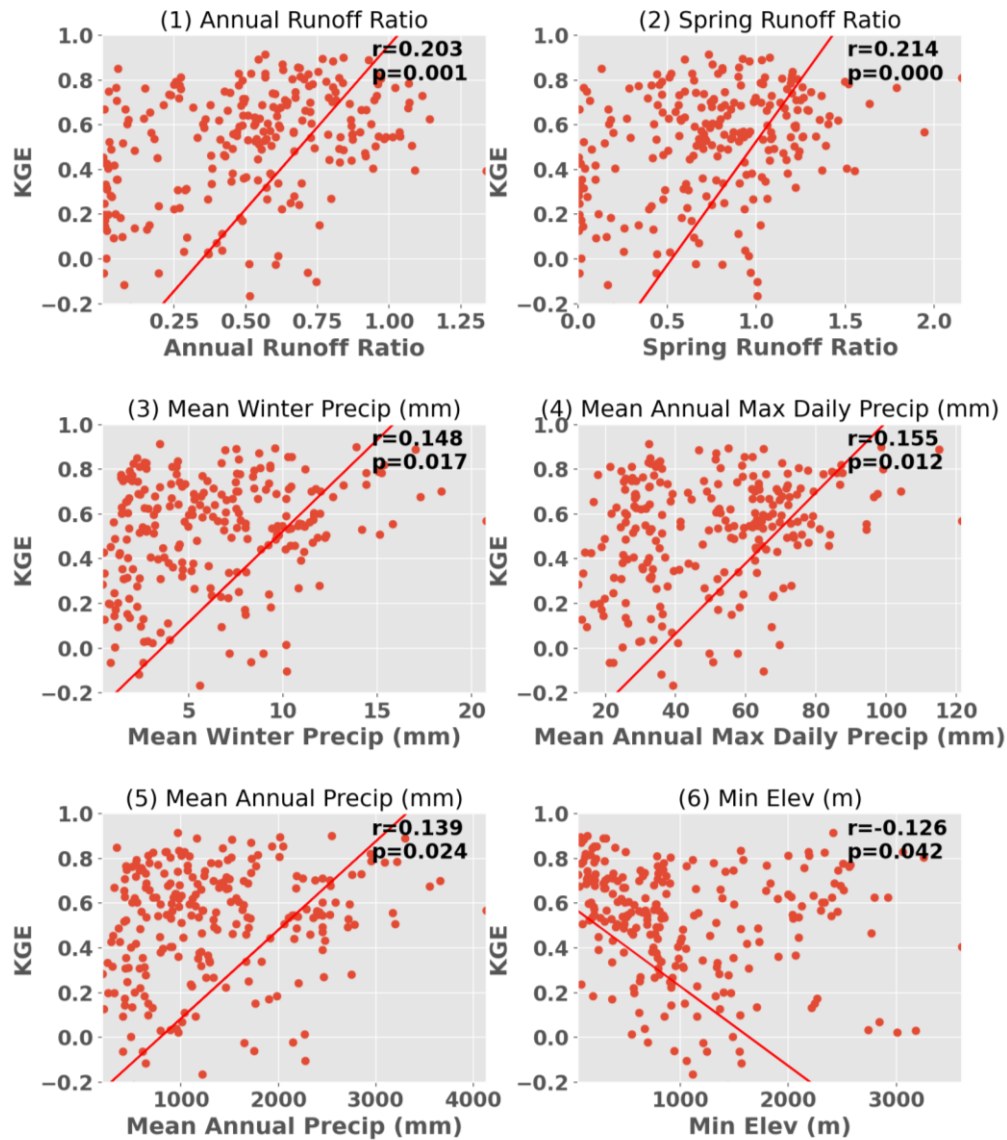


Figure 7. Scatterplot of Noah-MP KGE in relation to significantly correlated characteristics. Each subplot indicates the corresponding Pearson correlation coefficients and the P-value.

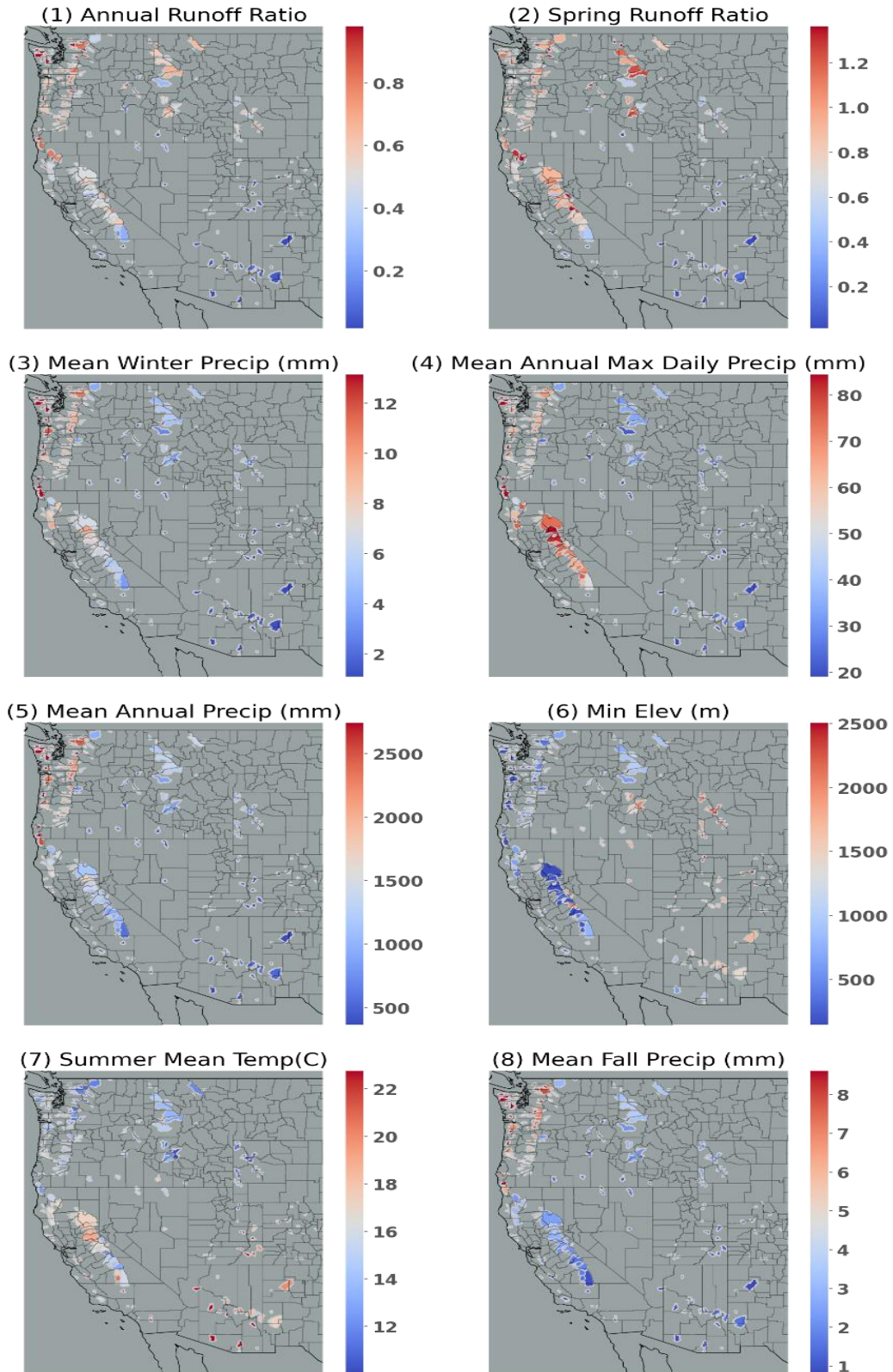


Figure 8. Spatial distribution of characteristics that are statistically significantly correlated with KGE. Note that all characteristics are significantly correlated with VIC KGE whereas only (1)-(6) are significantly correlated with Noah-MP KGE.

4. Regionalization

To distribute parameters from the calibration basins to the entire region, we used the donor-basin method as implemented in numerous previous studies (e.g., Arsenault and Brissette (2014); Poissant et al. (2017); Razavi and Coulibaly (2017); Gochis et al. (2019); Qi et al. (2021) and Bass et al. (2023). Following the calibration process, we regionalized the parameters from gauged to ungauged basins based on a mathematical assessment of the spatial and physical proximity between the gauged and ungauged basins. We considered two primary methods for implementing the donor basin approach. The first uses models calibrated to spatially continuous gridded runoff metrics (Beck et al. 2015; Yang et al. 2019). The second approach, which we ultimately adopted, calibrates models to individual gauges, then extends these parameters to ungauged basins, based either on a statistical or mathematical similarity measures (e.g., Arsenault and Brissette 2014; Razavi and Coulibaly 2017). Our preference for the second method was guided by a key limitation of the first approach, specifically it is limited to calibrating against runoff metrics, such as long-term mean flow and flow percentiles, rather than streamflow time series.

In the donor-basin method, an ungauged basin inherits its land surface parameters from the most similar gauged basin(s) (or the 'n' most similar gauged basins). Here, we evaluated the similarity or proximity between gauged and ungauged basins based on the similarity index SI as defined and used by Burn and Boorman (1993) and Poissant et al. (2017):

$$SI = \sum_{i=1}^k \frac{|X_i^G - X_i^U|}{\Delta X_i} \quad (1)$$

In Eq. 1, k stands for the total number of features considered, X_i^G represents the ith feature of the gauged basin G, X_i^U is the ith feature of a specific ungauged basin, and ΔX_i is the range of potential values for the ith feature, grounded in the data from the

gauged basins. This yields a unique value of SI for each gauged basin, contingent on the specific ungauged basin it is compared with. Typically, gauged basins that exhibit greater resemblance to the ungauged basin will have a smaller SI.

We assessed the donor-basin method's efficacy using a cross-validation approach, where each gauged basin was treated as ungauged one at a time. The pseudo-ungauged basin inherits its hydrological parameters from its three most similar gauged basins, determined by SI. The parameters inherited are a weighted average from the three donor basins. After testing one to five donor basins, we found that using three donors yielded the best results. Thus, every basin inherits parameters from the three most similar gauged basins in each simulation, offering a concise evaluation of the donor-basin method's regionalization performance.

We used 18 basin-specific features in the donor basin method, detailed in Table S1, calculated based on the forcings and parameters used in the study. For feature selection in the donor-basin method, we adopted an iterative approach, explained in detail in the following paragraph. Only basins with a KGE exceeding 0.3 were considered, following previous studies suggesting that inclusion of poorly performing basins can lower regionalization performance. We found that a KGE threshold of 0.3 resulted in a median performance improvement of 0.08 larger than did a KGE threshold of 0, hence it was chosen. After screening, 223 basins were utilized in VIC regionalization and 194 in Noah-MP regionalization. We note that the parameters used for calibration and the features used to determine the similarity index in the regionalization process are different. The physics that control the key hydrological processes of the two models are different, so we explored their best regionalization features separately.

To determine the most effective regionalization features from the 18 basin characteristics listed in Table S1, we employed a systematic iterative approach. The

first iteration includes 18 simulations, each of which incorporates one of the 18 features. The feature that yielded the greatest increase in the median KGE across all basins, based on leave-one-out cross validation, was then retained. In the second iteration, we conducted 17 simulations, each combining the retained feature from the first iteration with one of the remaining 17 features. This process was repeated iteratively, reducing the number of features considered in each subsequent round, until the addition of new features no longer resulted in an appreciable increase in median KGE. The sequence of features shown in Figure 9 (also shown in Table S1) indicated the importance of the features. This iterative approach ensured that each feature's individual and combined contribution to model performance was thoroughly assessed. It allowed us to identify a subset of features that, when used together, optimally improved model accuracy. We recognize the potential existence of inter-feature correlations that may exert a discernible influence on their collective efficacy when utilized in combination.

This procedure resulted in five features generated the best regionalization performance for VIC (longitude centroid, latitude centroid, maximum elevation, fall mean precipitation, and fall mean temperature). Three features were found to be best for Noah-MP (latitude centroid, longitude centroid, and drainage area) (see Figure 9). Among them, latitude and longitude are the common features that contribute the most to regionalization when using the similarity index method. This suggests that geographical similarities are the most important factor in parameter information transfer from gauged to ungauged basins.

Upon evaluating the performance of baseline, calibrated, and regionalized simulations, the respective median daily KGEs for the VIC model were found to be 0.41, 0.71, and 0.49. For the Noah-MP, these values were 0.38, 0.60, and 0.49 (refer to Figures 9 & S4). These metrics are for basins that have a calibrated KGE greater

than 0.3 only, resulting in higher median KGEs than for all 263 basins (See Figure 4). The KGE distribution also improved overall. It's noteworthy that the regionalization improvement relative to baseline is higher for Noah-MP than for VIC. While VIC's baseline and calibrated KGE skill distribution outperforms Noah-MP's, the differences between regionalized skills of Noah-MP and VIC are decreasing. We will explore more on this in the following section.

After optimizing the features and specific design of the donor-basin method, parameters were regionalized to 4816 ungauged USGS Hydrologic Unit Code (HUC) -10 basins across the WUS. HUCs are delineated and quality controlled by USGS using high-resolution DEMs. For each of the 4816 HUC-10 basins, we calculated a similarity index with the calibrated basins using the selected features. The three most similar basins were identified as donor basins, and their weighted average parameters were then adopted by the target HUC-10 basin. The final hydrologic parameters for both VIC and Noah-MP for all WUS HUC-10 basins are shown in Figures S5&6. The baseline HUC-10 parameters are shown in Figures S7&8.

Comparison of Figures S5-6 to Figures S7-8 makes it clear that the baseline model parameters lack accuracy, and exhibit significant spatial uniformity where large geographical regions share identical parameter values. For example, parameters such as *Ds* and *Soil_Depth1* in VIC show this uniformity. Furthermore, certain parameters, such as *SLOPE* and *REFKDT* in Noah-MP, remain invariant across all spatial domains, and don't reflect real-world conditions. Regionalization, improved the parameters, leading to increased accuracy and strengthening of region-specific characteristics.

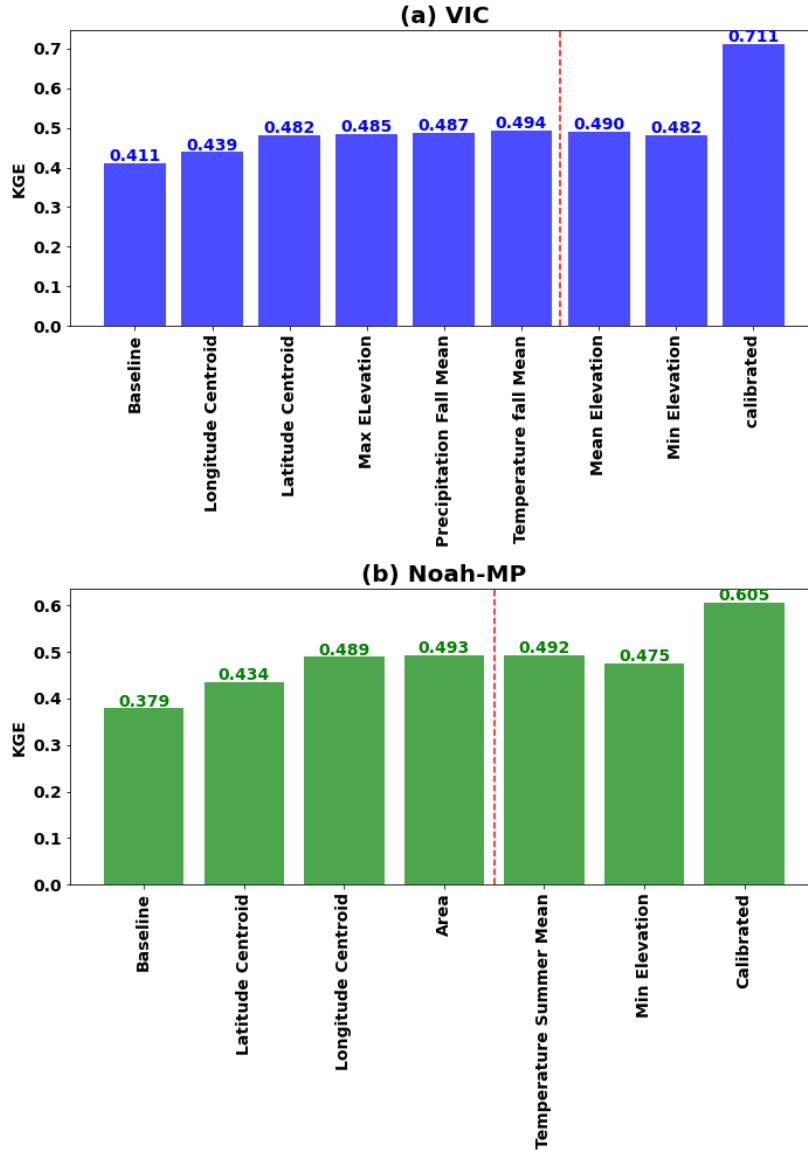


Figure 9. Best regionalization features for (a) VIC and (b) Noah-MP. The final regionalization to ungauged basins of the WUS incorporated all features up to the point marked by the red line since the addition of further features doesn't improve KGE.

5. Evaluation of calibration and regionalization skills

Our primary calibration objective was to enhance the accuracy of daily streamflow simulations. However, to ensure the versatility of our parameter sets for research related to both floods and dry conditions, we also evaluated the models' capabilities in reproducing high and low streamflow. To understand the capabilities of

the two models in reconstructing high and low streamflow, we assessed their performance across baseline, calibrated, and regionalized settings.

(a) Evaluation of high flow performance

We used the peaks-over-threshold (POT) method (Lang et al. 1999) to identify extreme streamflow events as in Su et al (2023) and Cao et al. (2019, 2020). We first applied the event independence criteria from USWRC (1982) to daily streamflow data to identify independent events. We set thresholds at each basin that resulted in 3 extreme events per year on average (denoted as POT3). After selecting the flood events over the study period based on the observation, we sorted the floods based on the return period and then calculated the KGE of baseline, calibrated and regionalized floods. Figure S9 displays the associated CDF plots. The median KGE for baseline floods in Noah-MP was 0.14, which rose to 0.37 post-calibration, and receded to 0.22 after regionalization. For VIC, the flood KGE started at 0.11, increased to 0.41 after calibration, and declined to 0.20 post-regionalization. As anticipated, these numbers are lower than (all) daily streamflow skill due to our calibration target being daily streamflow. Still, flood competencies experienced considerable enhancement, surpassing the Noah-MP KGE benchmark of -0.41 found by Knoben et al. (2019).

(b) Evaluation of low flow performance

(c) To assess low flow performance, we utilized the 7q10 metric. This hydrological statistic, commonly adopted in water resources management and environmental engineering, is the lowest 7-day average flow that occurs (on average) once every 10 years (EPA,2018). Scatterplots of 7q10 (Figure S10) showed high correlation between our model's simulated low flows and the observed data. Post-calibration, this alignment intensified. The VIC model tended to underestimate the low flows. After calibration, the median bias improved from -23.6% to -9.9%, and with regionalization, it was -11.7%.

In contrast, Noah-MP began with an 11.20% overestimation in the baseline, improved to 0.61% post-calibration, and was -9.5% after regionalization. The outcomes underline the proficiency of both models for low flow prediction, exhibiting enhanced competencies post-calibration and commendable performance after regionalization. Comparison of VIC and Noah-MP simulation skill

In Section 4, we demonstrated that while VIC's baseline and calibrated daily streamflow KGE skill distribution was better than Noah-MP's, the disparity was reduced following regionalization. We further explored the skill differences between the two models for baseline, calibrated, and regionalized parameters for different hydroclimatic conditions. Figure 10 shows the CDF of the daily streamflow KGE differences between VIC and Noah-MP across the study basins. The skill gap between VIC and Noah-MP generally narrows from baseline through calibrated to regionalized runs, although VIC outperforms Noah-MP in most of the basins for all three runs.

We further divided the study region into four different categories following Huang et al (2021): coastal snow dominated basins, coastal rain dominated, interior wet, and interior dry. In the baseline runs (Figure 10 and 11.1), VIC generally outperforms Noah-MP with a median KGE difference of 0.168, particularly in interior dry basins, and in some interior wet and coastal basins. Following calibration (Figure 10 and 11.2), the median KGE difference decreases to 0.126. VIC has superior performance in most of the basins, especially interior wet and coastal basins. In interior dry basins (mostly in the southeastern part of our domain), VIC's performance is similar to or worse than Noah-MP's. This discrepancy is attributable to more pronounced improvements in VIC after calibration in coastal and northern WUS, while Noah-MP shows greater improvements in the southeastern WUS (mostly dry interior). Post-regionalization (Figure 10 and 11.3), the KGE differences further

narrow to a median of 0.054, with VIC still outperforming Noah-MP in most coastal and interior wet basins. Nonetheless, VIC is inferior in a few interior dry basins scattered across WUS, where both models exhibit relatively low skill. This is also shown in Figure S11 CDFs which indicate that VIC's performance varies notably across the spectrum: it falls below Noah-MP at the lower end of the skill distribution. Conversely, VIC KGEs exceed those of Noah-MP in areas where its skill is strongest. Across all basins collectively, VIC outperforms Noah-MP post regionalization as evidenced by higher VIC median skill (Figure 10 inset).

We also evaluated the performance of the two models after regionalization in simulating annual average flows, flood flows (POT3), and low flows (measured as 7q10). The results (see Figures S12 and S13) show that VIC outperforms Noah-MP in simulating annual mean streamflow (Figure S12) and (in most cases) floods (Figure S13). Conversely, Noah-MP generally performs better in simulating low flows (Figure S10).

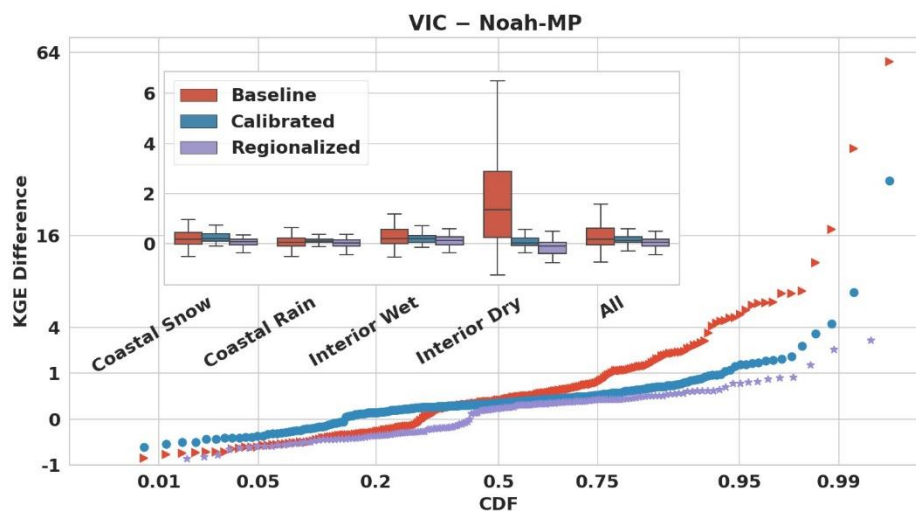


Figure 10. Cumulative distribution function (CDF) plot of the daily streamflow KGE differences between VIC and Noah-MP in the study basins for baseline, calibrated and regionalized runs. The inset figure shows boxplots of KGE differences for four

different categories: coastal snow dominated basins (54 basins), coastal rain dominated basins (103 basins), interior wet basins (53 basins), and interior dry basins (53 basins). We also show all basins collectively (263 total) for reference purposes.

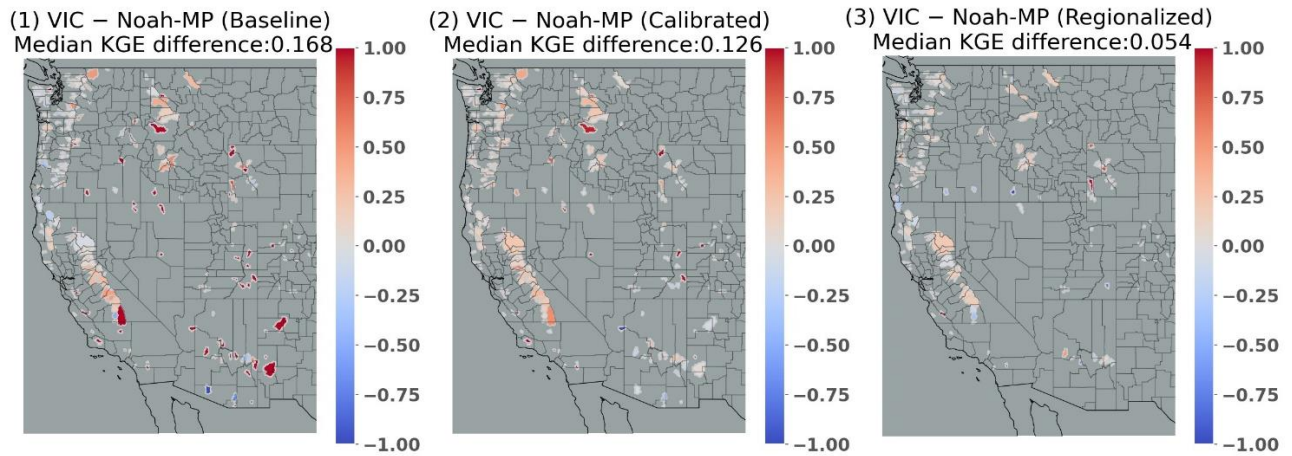


Figure 11. Map of the daily streamflow KGE differences between VIC and Noah-MP in the study basins for (1) baseline, (2) calibrated and (3) regionalized runs.

(d) Comparison of post-regionalization and post-calibration performance

We further analyzed the performance differences between the regionalized and calibrated runs for each model. As depicted in Figure 12, both VIC and Noah-MP have declining skill for post-regionalization relative to post-calibration runs, with VIC demonstrating a more pronounced decrease, reflected in a median KGE difference of -0.199, compared to -0.117 for Noah-MP. For both models, coastal basins and interior wet basins tend to have smaller skill decreases from post-calibration to post-regionalization; and interior dry basins have the largest skill decreases. VIC has greater decreases than Noah-MP in most basins. The most significant drops in performance generally occur in basins where baseline skills are low, yet post-calibration skills are relatively high.

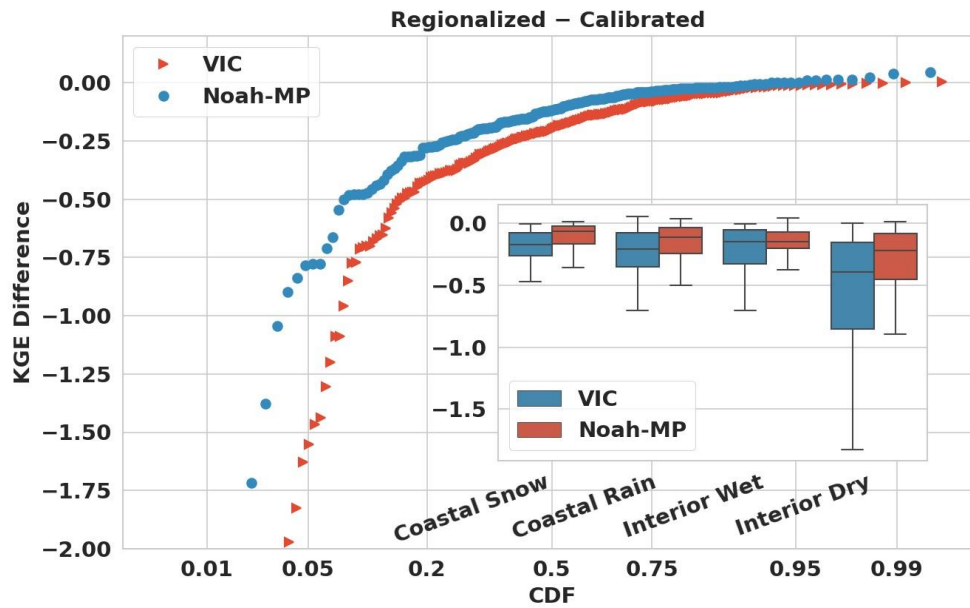


Figure 12. CDF of differences of daily streamflow skill between regionalized and calibrated for VIC and Noah-MP. The inset figure summarizes KGE difference distributions for the same four categories as the inset in Figure 10.

6. Discussion

We summarize our key accomplishments in calibrating the two hydrological models, examine our approach to choosing calibration objective functions and metrics, and we consider lessons learned in model regionalization.

(a) Improved parameter sets

We generated calibrated parameter sets for the VIC and Noah-MP hydrological models at $1/16^\circ$ latitude-longitude scale across WUS. These calibrated parameter sets are intended to facilitate the use of the two models for climate change and water investigations across the region, among other applications. Our focus on calibrating daily streamflow aligns with common practice in hydrology, providing a comprehensive representation of catchment hydrology dynamics which should enhance future understanding of hydrological phenomena and their spatial variations across the region.

(b) Selection of calibration objective function

We used objective functions based on streamflow observations. We chose this approach due to its applicability elsewhere, given the widespread accessibility of streamflow observations as compared to alternative metrics such as soil moisture or evapotranspiration (Demaria et al., 2007; Gao et al., 2018; Troy et al., 2008; Yadav et al., 2007). While we acknowledge the potential of remote sensing products like MODIS, SMAP, SMOS, ESA, and ALEXI to improve calibration efforts, especially for variables like actual evapotranspiration (AET) and soil moisture (SM), we were limited by the scarcity of observations for these variables. Future studies could, nonetheless, leverage from the methods we've employed to incorporate additional variables into the objective functions we used.

(c) Selection of calibration metric

We used the KGE metric applied to daily streamflow, which we chose for its ability to address bias, correlation, and variability simultaneously (Knoben et al., 2019). We also evaluated NSE and BIAS metrics, and found substantial improvements in both models' performance after calibration when these metrics were used in place of KGE (See Figures S2-3). Our assessment of high and low flow reconstruction in Section 5 further validated our generated parameter sets. While we used a single objective function due to data and computing constraints, incorporating multiple objective functions is feasible in principle.

(d) Regionalization possibilities

We calibrated model parameters directly for individual basins, considering their unique hydrological features, and then transferred these calibrated parameters to similar basins based on similarity assessments. Alternative parameter transfer strategies could be used within the same framework we employed (e.g., pedo-transfer functions, e.g. Imhoff et al., 2020) or multiscale parameter regionalization (e.g.

Schweppe et al.,2022). We do note that our regionalization approach facilitates the transfer of calibrated parameters to comparable regions, which could be explored in future research.

7. Conclusions

Our intent was to develop a regional parameter estimation strategy for the VIC and Noah-MP land surface schemes, and to apply it across the WUS region at the HUC-10 catchment scale. We've described what we believe is a robust framework that can be applied in future hydrological and climate change studies across the WUS, and is applicable to other regions as well. Our key findings and conclusions are:

- a) Our catchment scale calibration of the two models to 263 sites across WUS resulted in major improvements in the performance of both models relative to a priori parameters, but performance improvement was greatest for Noah-MP – although this may be in part because VIC a priori parameters benefitted from prior calibration and hence resulted in better baseline performance than did a priori Noah-MP.
- b) Both models performed best in more humid basins, mainly in the Pacific Northwest and central to northern CA where runoff ratios are high. This is consistent with previous results (e.g. Bass et al.,2023).
- c) Post-calibration regional model performance improved for both models in most areas, especially where the baseline KGE was low, such as southern CA and the southeastern part of the study region.
- d) VIC performance across all calibration basins was mostly better than for Noah-MP. However, Noah-MP performance benefitted more from regionalization than did VIC, and ultimately post-regionalization VIC performance was only slightly superior to that of Noah-MP. When partitioned into hydroclimatic categories, VIC outperforms Noah-MP in all

but interior dry basins following regionalization, where Noah-MP is better.

- e) Post-regionalization, both VIC and Noah-MP performance declines in comparison with the calibrated run, with declines more pronounced for VIC. The performance degradation is greatest in interior dry basins for both models.
- f) VIC outperforms Noah-MP in simulating annual mean streamflow and flood simulations in most cases. Conversely, Noah-MP performs better for low flows. These results should provide guidance for selecting the most appropriate model depending on the hydrological condition being analyzed.

Data Availability statement

The Livneh (2013) forcings are available at <http://livnehpublicstorage.colorado.edu:81/Livneh.2013.CONUS.Dataset/>. The extended forcings used in this study are available at <ftp://livnehpublicstorage.colorado.edu/public/sulu>. The results are available online at <https://figshare.com/s/66fe8305bff516e80f6f>.

Author contribution

LS and DL conceptualized the study. LS generated the dataset and analysis with support of DL, MP and BB. LS drafted the manuscript with support of DL.

Competing interests. The contact author has declared that none of the authors has any competing interests.

References

- Adam, J.C. and Lettenmaier, D.P.: Adjustment of global gridded precipitation for systematic bias, *J. Geophys. Res.*, 108(D9), 1-14, doi:10.1029/2002JD002499, 2003.
- Adam, J.C., Clark, E.A. , Lettenmaier, D.P. and Wood, E.F.: Correction of Global Precipitation Products for Orographic Effects, *J. Clim.*, 19(1), 15-38, doi: 10.1175/JCLI3604.1, 2006.
- Anghileri, D., Voisin, N., Castelletti, A., Pianosi, F. , Nijssen, B. and Lettenmaier, D.P.: Value of Long-Term Streamflow Forecasts to Reservoir Operations for Water Supply in Snow-Dominated River Catchments. *Water Resources Research* 52: 4209–25, 2016.
- Arsenault, R., and Brissette, F. P.: Continuous streamflow prediction in ungauged basins: The effects of equifinality and parameter set selection on uncertainty in regionalization approaches. *Water Resour. Res.*, 50, 6135–6153, <https://doi.org/10.1002/2013WR014898>, 2014.
- Bass, B., Rahimi, S., Goldenson, N., Hall, A., Norris, J. and Lebow, Z.J.: Achieving Realistic Runoff in the Western United States with a Land Surface Model Forced by Dynamically Downscaled Meteorology. *Journal of Hydrometeorology*, 24(2), 269-283, 2023.
- Beck, H. E., Roo, A. de and van Dijk, A. I. J. M.: Global maps of streamflow characteristics based on observations from several thousand catchments. *J. Hydrometeor.*, 16, 1478–1501, <https://doi.org/10.1175/JHM-D-14-0155.1>, 2015.
- Bennett, A. R., Hamman, J. J. and Nijssen, B.: MetSim: A Python package for estimation and disaggregation of meteorological data. *J. Open Source Software*, 5, 2042, <https://doi.org/10.21105/joss.02042>, 2020.
- Beven, K.: Changing ideas in hydrology-the case of physically-based models. *Journal*

725 of Hydrology, 105(1-2), 157–172. [https://doi.](https://doi.org/10.1016/0022-1694(89)90101-7)
 726 [org/10.1016/0022-1694\(89\)90101-7](https://doi.org/10.1016/0022-1694(89)90101-7), 1989.
 727 Bohn, T. J., Livneh, B., Oyster, J. W., Running, S. W., Nijssen, B. and Lettenmaier, D.
 728 P.: Global evaluation of MTCLIM and related algorithms for forcing of
 729 ecological and hydrological models. Agric. For. Meteor., 176, 38–49,
 730 <https://doi.org/10.1016/j.agrformet.2013.03.003>, 2013.
 731 Burn, D. H., and Boorman, D. B.: Estimation of hydrological parameters at ungauged
 732 catchments. J. Hydrol., 143, 429–454, [https://doi.org/10.1016/0022-](https://doi.org/10.1016/0022-1694(93)90203-L)
 733 [1694\(93\)90203-L](https://doi.org/10.1016/0022-1694(93)90203-L), 1993.
 734 Cai, X., Yang, Z.-L. , David, C. H., Niu, G.-Y. and Rodell, M.: Hydrological
 735 evaluation of the Noah-MP land surface model for the Mississippi River Basin. J.
 736 Geophys. Res. Atmos., 119, 23–38, <https://doi.org/10.1002/2013JD020792>, 2014.
 737 California Department of Water Resources: California data exchange center: Daily
 738 full natural flow for December 2022. California Department of Water Resources,
 739 accessed 1 October 2021, [https://cdec.water.ca.gov/reportapp/javareports?name=](https://cdec.water.ca.gov/reportapp/javareports?name=FNF)
 740 [FNF](https://cdec.water.ca.gov/reportapp/javareports?name=FNF), 2021.
 741 Cao, Q., Mehran, A. , Ralph, F. M. and Lettenmaier, D. P.: The role of hydrological
 742 initial conditions on atmospheric river floods in the Russian River basin. J.
 743 Hydrometeor., 20, 1667–1686, <https://doi.org/10.1175/JHM-D-19-0030.1>, 2019.
 744 Cao, Q., Gershunov, A., Shulgina, T., Ralph, F. M. , Sun, N. and Lettenmaier, D. P.:
 745 Floods due to atmospheric rivers along the U.S. West Coast: The role of
 746 antecedent soil moisture in a warming climate. J. Hydrometeor., 21, 1827–1845,
 747 <https://doi.org/10.1175/JHM-D-19-0242.1>, 2020.
 748 Castiglioni, S., Lombardi, L., Toth, E. , Castellarin, A. and Montanari, A.: Calibration
 749 of rainfall-runoff models in ungauged basins: A regional maximum likelihood
 750 approach. Advances in Water Resources, 33(10), 1235–1242.

751 <https://doi.org/10.1016/j.advwatres.2010.04.009>, 2010.

752 Chen, F., and Dudhia, J.: Coupling an advanced land surface–hydrology model with
 753 the Penn State–NCAR MM5 modeling system. Part I: Model implementation
 754 and sensitivity. *Mon. Wea. Rev.*, 129, 569–585, [https://doi.org/10.1175/1520-](https://doi.org/10.1175/1520-0493(2001)129<0569:CAALSH>2.0.CO;2)
 755 [0493\(2001\)129<0569:CAALSH>2.0.CO;2](https://doi.org/10.1175/1520-0493(2001)129<0569:CAALSH>2.0.CO;2), 2001.

756 Chen, F., and Coauthors: Modeling of land-surface evaporation by four schemes and
 757 comparison with FIFE observations. *J. Geophys. Res.*, 101, 7251–7268,
 758 <https://doi.org/10.1029/95JD02165>, 1996.

759 Cosby, B.J., Hornberger, G.M., Clapp, R.B. and Ginn, T.: A statistical exploration of
 760 the relationships of soil moisture characteristics to the physical properties of soils.
 761 *Water resources research*, 20(6), 682–690, 1984.

762 Demaria, E. M., Nijssen, B., & Wagener, T.: Monte Carlo sensitivity analysis of land
 763 surface parameters using the Variable Infiltration Capacity model. *Journal of*
 764 *Geophysical Research*, 112, D11113. <https://doi.org/10.1029/2006JD007534>,
 765 2007.

766 Dembélé M, Hrachowitz M, Savenije H.H, Mariéthoz G, Schaefli B.: Improving the
 767 predictive skill of a distributed hydrological model by calibration on spatial
 768 patterns with multiple satellite data sets. *Water resources research*,
 769 Jan;56(1):e2019WR026085, <https://doi.org/10.1029/2019WR026085>, 2020

770 Demirel, M. C., Mai, J., Mendiguren, G., Koch, J., Samaniego, L., and Stisen, S.:
 771 Combining satellite data and appropriate objective functions for improved spatial
 772 pattern performance of a distributed hydrologic model, *Hydrol. Earth Syst. Sci.*,
 773 22, 1299–1315, <https://doi.org/10.5194/hess-22-1299-2018>, 2018.

774 Dickinson, R. E., Henderson-Sellers, A. & Kennedy, P. J.: Biosphere–Atmosphere
 775 Transfer Scheme (BATS) version 1e as coupled to the NCAR Community
 776 Climate Model. NCAR Tech. Note TN383+STR, NCAR, 1993.

777 Duan, Q., Sorooshian, S. and Gupta, V. : Effective and efficient global optimization
 778 for conceptual rainfall-runoff models. *Water Resour. Res.*, 28, 1015–1031,
 779 [https://doi.org/ 10.1029/91WR02985](https://doi.org/10.1029/91WR02985), 1992.

780 Environmental Protection Agency (EPA) Office of Water: Low Flow Statistics Tools:
 781 A How-To Handbook for NPDES Permit Writers. EPA-833-B-18-001, 2018.

782 Falcone, J.: GAGES-II: Geospatial attributes of gages for evaluating streamflow. U.S.
 783 Geological Survey, accessed 1 April 2021,
 784 [https://water.usgs.gov/GIS/metadata/usgswrd/XML/ gagesII_Sept2011.xml](https://water.usgs.gov/GIS/metadata/usgswrd/XML/gagesII_Sept2011.xml), 2011.

785 Fisher, R.A. and Koven, C.D.: Perspectives on the future of land surface models and
 786 the challenges of representing complex terrestrial systems. *Journal of Advances*
 787 *in Modeling Earth Systems*, 12(4), p.e2018MS001453, 2020.

788 Franchini, M., Galeati, G. and Berra S.: Global optimization techniques for the
 789 calibration of conceptual rainfall-runoff models, *Hydrol. Sci. J.*, 43, 443 – 458,
 790 1998.

791 Gao, H., Birkel, C., Hrachowitz, M., Tetzlaff, D., Soulsby, C., & Savenije, H. H.
 792 (2018). A simple topography-driven, calibration-free runoff generation model.
 793 *Hydrology and earth system sciences discussions.*,1–42.
 794 <https://doi.org/10.5194/hess-2018-141>

795 Gochis, D. and Coauthors: Overview of National Water Model Calibration: General
 796 strategy and optimization. National Center for Atmospheric Research, accessed 1
 797 January 2023, 30 pp.,
 798 [https://ral.ucar.edu/sites/default/files/public/9_RafieeiNasab_CalibOverview_CU](https://ral.ucar.edu/sites/default/files/public/9_RafieeiNasab_CalibOverview_CU_AHSI_Fall019_0.pdf)
 799 [AHSI_Fall019_0.pdf](https://ral.ucar.edu/sites/default/files/public/9_RafieeiNasab_CalibOverview_CU_AHSI_Fall019_0.pdf), 2019.

800 Gong, W., Duan, Q., Li, J., Wang, C., Di, Z., Dai, Y., et al.: Multi-objective parameter
 801 optimization of common land model using adaptive surrogate modeling.
 802 *Hydrology and Earth System Sciences*, 19(5), 2409–2425.

803 <https://doi.org/10.5194/hess-19-2409-2015>, 2015.

804 Gou, J., Miao, C., Duan, Q., Tang, Q., Di, Z., Liao, W., Wu, J. and Zhou, R.:

805 Sensitivity analysis-based automatic parameter calibration of the VIC model for

806 streamflow simulations over China. *Water Resources Research*, 56(1),

807 e2019WR025968, 2020.

808 Gupta, H. V., et al.: Decomposition of the mean squared error and NSE performance

809 criteria: Implications for improving hydrological modelling. *Journal of*

810 *Hydrology*, 377, 80-91,2009.

811 Holtzman, N.M., Pavelsky, T.M., Cohen, J.S., Wrzesien, M.L. and Herman, J.D.:

812 Tailoring WRF and Noah-MP to improve process representation of Sierra

813 Nevada runoff: Diagnostic evaluation and applications. *Journal of Advances in*

814 *Modeling Earth Systems*, 12(3), p.e2019MS001832, 2020.

815 Huang, H., Fischella, M., Liu, Y. , Ban, Z. , Fayne, J. , Li, D. , Cavanaugh, K. and

816 Lettenmaier, D.P.: Changes in mechanisms and characteristics of Western U.S.

817 floods over the last sixty years. *Geophysical Research Letters*, 49, DOI:

818 10.1029/2021GL097022, 2021

819 Hussein, A.: Process-based calibration of WRF-hydro model in unregulated

820 mountainous basin in Central Arizona. M.S. thesis, Ira A. Fulton Schools of

821 Engineering, Arizona State University, 110 pp.,

822 [https://keep.lib.asu.edu/_flysystem/fedora/](https://keep.lib.asu.edu/_flysystem/fedora/c7/224690/Hussein_asu_0010N_19985.pdf)

823 [c7/224690/Hussein_asu_0010N_19985.pdf](https://keep.lib.asu.edu/_flysystem/fedora/c7/224690/Hussein_asu_0010N_19985.pdf), 2020.

824 Imhoff, R.O., Van Verseveld, W.J., Van Osnabrugge, B. and Weerts, A.H.: Scaling

825 point-scale (pedo) transfer functions to seamless large-domain parameter

826 estimates for high-resolution distributed hydrologic modeling: An example for

827 the Rhine River. *Water Resources Research*, 56(4), p.e2019WR026807,2020.

828 Fisher, R. A. and Koven, C. D. : Perspectives on the Future of Land Surface Models

and the Challenges of Representing Complex Terrestrial Systems. *Journal of Advances in Modeling Earth Systems*, 12(4), <https://doi.org/10.1029/2018MS001453>, 2020. Kimball, J. S., Running, S. W. and Nemani, R. R.: An improved method for estimating surface humidity from daily minimum temperature. *Agric. For. Meteorol.*, 85, 87–98, [https://doi.org/10.1016/S0168-1923\(96\)02366-0](https://doi.org/10.1016/S0168-1923(96)02366-0), 1997.

Lahmers, T.M., et al.: Evaluation of NOAA national water model parameter calibration in semiarid environments prone to channel infiltration. *Journal of Hydrometeorology*, 22(11), 2939-2969, 2021.

Li, D., Lettenmaier, D. P., Margulis, S. A. and Andreadis, K.: The role of rain-on-snow in flooding over the conterminous United States. *Water Resour. Res.*, 55, 8492–8513, <https://doi.org/10.1029/2019WR024950>, 2019.

Liang, X., Lettenmaier, D. P., Wood, E. F. and Burges S. J. : A simple hydrologically based model of land surface water and energy fluxes for general circulation models, *J. Geophys. Res.*, 99(D7), 14415–14428, doi:10.1029/94JD00483, 1994.

Livneh B, Rosenberg, E.A., Lin, C., Nijssen, B., Mishra, V., Andreadis, K., Maurer, E.P. and Lettenmaier, D.P.: A long-term hydrologically based data set of land surface fluxes and states for the conterminous United States: Updates and extensions, *Journal of Climate*, doi:10.1175/JCLI-D-12-00508.1, 2013.

Maidment, D.R.: Conceptual Framework for the National Flood Interoperability Experiment. *Journal of the American Water Resources Association* 53: 245–57, 2017.

Mascaro, G., Hussein, A., Dugger, A. and Gochis, D.J.: Process-based calibration of WRF-Hydro in a mountainous basin in southwestern US. *Journal of the American Water Resources Association*, 59(1), 49-70, 2023.

Mendoza, P.A., Clark, M.P., Mizukami, N., Newman, A.J., Barlage, M., Gutmann,

855 E.D., Rasmussen, R.M., Rajagopalan, B., Brekke, L.D. and Arnold, J.R.: Effects
856 of hydrologic model choice and calibration on the portrayal of climate change
857 impacts. *Journal of Hydrometeorology*, 16(2), 762-780, 2015.

858 Miller, D.A. and White, R.A.: A conterminous United States multilayer soil
859 characteristics dataset for regional climate and hydrology modeling. *Earth*
860 *interactions*, 2(2), pp.1-26, 1998.

861 Mizukami, N., Clark, M. P., Newman, A. J., Wood, A. W., Gutmann, E. D., Nijssen,
862 B. , Rakovec, O. and Samaniego, L. :Towards seamless large-domain parameter
863 estimation for hydrologic models. *Water Resour. Res.*, 53, 8020–8040, [https://](https://doi.org/10.1002/2017WR020401)
864 doi.org/10.1002/2017WR020401, 2017.

865 Naeini, M.R., Analui, B., Gupta, H.V., Duan, Q. and Sorooshian, S.. Three decades of
866 the Shuffled Complex Evolution (SCE-UA) optimization algorithm: Review and
867 applications. *Scientia Iranica*, 26(4), 2015-2031, 2019.

868 Natural Resources Conservation Service: SNOTEL (Snow Telemetry) Data. USDA.
869 <https://www.nrcs.usda.gov/wps/portal/wcc/home/>, 2023.

870 Niu, G.-Y., Yang, Z.-L. , Dickinson, R. E. , Gulden, L. E. and Su, H.: Development of
871 a simple groundwater model for use in climate models and evaluation with
872 gravity recovery and climate experiment data. *J. Geophys. Res.*, 112, D07103,
873 <https://doi.org/10.1029/2006JD007522>, 2007.

874 Niu, G. Y., Yang, Z. L., Dickinson, R. E., & Gulden, L. E.: A simple
875 TOPMODEL-based runoff parameterization (SIMTOP) for use in global climate
876 models. *Journal of Geophysical Research: Atmospheres*, 110(D21), 2005.

877 Niu, G.-Y., and Coauthors: The community Noah land surface model with
878 multiparameterization options (Noah-MP): 1. Model description and evaluation
879 with local-scale measurements. *J. Geophys. Res.*, 116, D12109,
880 <https://doi.org/10.1029/2010JD015139>, 2011.

881 NOAA (National Oceanic and Atmospheric Administration): National Water Model:
882 Improving NOAA's Water Prediction Services, 2016.

883 Oubeidillah, A. A., Kao, S.-C., Ashfaq, M. , Naz, B. S. and Tootle, G.: A large-scale,
884 high-resolution hydrological model parameter data set for climate change impact
885 assessment for the conterminous US. Hydrology and Earth System Sciences,
886 18(1), 67–84. [https://doi.org/ 10.5194/hess-18-67-2014](https://doi.org/10.5194/hess-18-67-2014), 2014.

887 Prata, A.J.: A new long-wave formula for estimating downward clear-sky radiation at
888 the surface. Quarterly Journal of the Royal Meteorological Society, 122(533),
889 1127-1151, 1996.

890 Poissant, D., Arsenault, A. and Brissette, F. : Impact of parameter set dimensionality
891 and calibration procedures on streamflow prediction at ungauged catchments. J.
892 Hydrol. Reg. Stud., 12,220–237, <https://doi.org/10.1016/j.ejrh.2017.05.005>, 2017.

893 Qi, W.Y., Chen, J. , Li, L. , Xu, C.-Y. , Xiang, Y.-h. , Zhang, S.-B. and Wang, H.-M.:
894 Impact of the number of donor catchments and the efficiency threshold on
895 regionalization performance of hydrological models. J. Hydrol., 601, 126680,
896 <https://doi.org/10.1016/j.jhydrol.2021.126680>, 2021.

897 Raff, D., Brekke, L. , Werner, K. , Wood, A. and White. K.: Short-Term Water
898 Management Decisions: User Needs for Improved Climate, Weather, and
899 Hydrologic Information. U.S. Bureau of Reclamation.
900 <https://www.usbr.gov/research/st/roadmaps/WaterSupply.pdf>, 2013.

901 Razavi, T., and Coulibaly, P.: An evaluation of regionalization and watershed
902 classification schemes for continuous daily streamflow prediction in ungauged
903 watersheds. Can. Water Resour. J., 42,2–20,
904 <https://doi.org/10.1080/07011784.2016.1184590>, 2017.

905 Rajsekhar, D., Singh, V.P. and Mishra, A.K., 2015. Hydrologic drought atlas for Texas.
906 Journal of Hydrologic Engineering, 20(7), p.05014023.

907 Schaake, J. C., Koren, V. I., Duan, Q.-Y., Mitchell, K., & Chen, F.: Simple water
 908 balance model for estimating runoff at different spatial and temporal scales.
 909 Journal of Geophysical Research, 101(D3), 7461–7475.
 910 <https://doi.org/10.1029/95JD02892>, 1996.

911 Schaperow J.R, Li, D., Margulis, S.A., Lettenmaier D.P. :A near-global, high
 912 resolution land surface parameter dataset for the variable infiltration capacity
 913 model. Scientific Data. Aug 11;8(1):216, 2021.

914 Schweppe, R., Thober, S., Müller, S., Kelbling, M., Kumar, R., Attinger, S., and
 915 Samaniego, L.: MPR 1.0: a stand-alone multiscale parameter regionalization tool
 916 for improved parameter estimation of land surface models, Geosci. Model Dev.,
 917 15, 859–882, <https://doi.org/10.5194/gmd-15-859-2022>, 2022.

918 Sharma, P. and Machiwal, D.: Streamflow forecasting: overview of advances in data-
 919 driven techniques. Advances in Streamflow Forecasting,1-50.
 920 <https://doi.org/10.1016/B978-0-12-820673-7.00013-5>, 2021

921 Shi, X., Wood, A.W. and Lettenmaier, D.P. : How essential is hydrologic model
 922 calibration to seasonal streamflow forecasting? Journal of Hydrometeorology,
 923 9(6), 1350-1363, 2008.

924 Sofokleous, I., Bruggeman, A., Camera, C. and Eliades, M.: Grid-based calibration of
 925 the WRF-Hydro with Noah-MP model with improved groundwater and
 926 transpiration process equations. Journal of Hydrology, 617, 128991 , 2023

927 Su, L., Cao, Q. , Xiao, M., Mocko, D. M., Barlage, M. , Li, D. , Peters-Lidard, C. D.
 928 and Lettenmaier, D. P.: Drought variability over the conterminous United States
 929 for the past century. J. Hydrometeor., 22, 1153–1168,
 930 <https://doi.org/10.1175/JHM-D-20-0158.1>, 2021.

931 Su, L., Cao, Q. , Shukla, S., Pan, M. and Lettenmaier, D.P.: Evaluation of Subseasonal
 932 Drought Forecast Skill over the Coastal Western United States. Journal of

Hydrometeorology, 24(4), 709-726, 2023.

Tangdamrongsub, N.: Comparative Analysis of Global Terrestrial Water Storage Simulations: Assessing CABLE, Noah-MP, PCR-GLOBWB, and GLDAS Performances during the GRACE and GRACE-FO Era. *Water*, 15(13), p.2456, 2023.

Thornton, P. E., and Running, S. W.: An improved algorithm for estimating incident daily solar radiation from measurements of temperature, humidity, and precipitation. *Agric. For. Meteorol.*, 93, 211–228, [https://doi.org/10.1016/S0168-1923\(98\)00126-9](https://doi.org/10.1016/S0168-1923(98)00126-9), 1999.

Tolson, B. A., and Shoemaker, C. A.: Dynamically dimensioned search algorithm for computationally efficient watershed model calibration. *Water Resour. Res.*, 43, W01413, <https://doi.org/10.1029/2005WR004723>, 2007.

Troy, T. J., Wood, E. F. and Sheffield, J.: An efficient calibration method for continental-scale land surface modeling. *Water Resources Research*, 44, W09411. <https://doi.org/10.1029/2007WR006513>, 2008

USWRC: Guidelines for determining flood flow frequency. Bulletin 17B of the Hydrology Subcommittee, 183 pp., https://water.usgs.gov/osw/bulletin17b/dl_flow.pdf, 1982.

Yang, Y., Pan, M., Beck, H.E. , Fisher, C.K., Beighley, R.E. , Kao, S.C. , Hong, Y. and Wood, E.F.: In quest of calibration density and consistency in hydrologic modeling: Distributed parameter calibration against streamflow characteristics. *Water Resources Research*, 55(9), 7784-7803, 2019.

Yadav, M., Wagener, T., & Gupta, H. (2007). Regionalization of constraints on expected watershed response behavior for improved predictions in ungauged basins. *Advances in Water Resources*, 30(8), 1756–1774. <https://doi.org/10.1016/j.advwatres.2007.01.005>

959 Zheng, H., Yang, Z.-L. , Lin, P. , Wei, J. , Wu, W.-Y., Li, L. , Zhao, L. and Wang, S.:
960 On the sensitivity of the precipitation partitioning into evapotranspiration and
961 runoff in land surface parameterizations. Water Resour. Res., 55, 95–111,
962 <https://doi.org/10.1029/2017WR022236>, 2019.

963 Zink M, Mai J, Cuntz M, Samaniego L. Conditioning a hydrologic model using
964 patterns of remotely sensed land surface temperature. Water Resources Research.
965 2018 Apr;54(4):2976-98.

966